Available online at www.sciencedirect.com
SCIENCE DIRECT®
PERGAMON
International Journal of Heat and Mass Transfer 46 (2003) 2519–2525
International Journal of HEAT and MASS TRANSFER
www.elsevier.com/locate/ijhmt

Friction factors in smooth trapezoidal silicon microchannels with different aspect ratios

H.Y. Wu [a,b], Ping Cheng [a,*]

[a] *Department of Mechanical Engineering, Hong Kong University of Science and Technology, Kowloon, Hong Kong*
[b] *School of Mechanical and Power Engineering, Shanghai Jiao Tong University, Shanghai, PR China*

Received 3 January 2003; received in revised form 15 February 2003

Abstract

An experiment has been conducted to measure the friction factor of laminar flow of deionized water in *smooth* silicon microchannels of trapezoidal cross-section with hydraulic diameters in the range of 25.9–291.0 μm. It is shown that the friction constant of these microchannels is greatly influenced by the cross-sectional aspect ratio, W_b/W_t. Based on the 334 data points, a correlation equation for the friction constant of a fully developed laminar flow of water in these microchannels is obtained in terms of the cross-sectional aspect ratio. The experimental data is found to be in good agreement with an existing analytical solution for an incompressible, fully developed, laminar flow under no-slip boundary condition. It is confirmed that the Navier–Stokes equations are still valid for the laminar flow of deionized water in smooth silicon microchannels having hydraulic diameter as small as 25.9 μm. For smooth channels with larger hydraulic diameters of 103.4–291.0 μm, transition from laminar to turbulent flow is found at $Re = 1500$–2000.

1. Introduction

In the past decade, a number of papers have reported pressure drop data on laminar flow of liquids and gases inside microchannels [1–6]. As pointed out by Pfund et al. [6], some of these authors conducted their experiments in microchannels of non-circular shape, but they compared their pressure drop data with the classical values $f\,Re = 16$ or 64 for a circular pipe. Based on these comparisons, others made the erroneous conclusions that Navier–Stokes equations may not be valid in microchannels. Recently, Ma and Peterson [7] obtained an analytical solution for the friction factor of a laminar incompressible flow in microchannels of irregular cross-section with two arbitrary boundaries. The solution was obtained based on the Navier–Stokes equations under the assumption of a fully developed laminar flow with no-slip boundary condition. However, it is uncertain whether this analytical solution is applicable to microchannels of trapezoidal cross-section that are widely used in many silicon-based microsystems. This is because the analytical solution is based on the Navier–Stokes equation with no-slip boundary condition that may not be valid in microscale.

In this paper, an extensive and careful experimental investigation has been carried out on the pressure drop of a laminar flow of water through *smooth* trapezoidal silicon microchannels with different cross-sectional aspect ratios. The excellent agreement between the experimental results with Ma and Peterson's analytical solution confirms that (i) the shape of the cross-sectional area has a great influence on the friction constant of a laminar flow of water inside the ⟨1 0 0⟩ silicon microchannels, and (ii) Navier–Stokes equations are valid for laminar flow of water in smooth silicon microchannels having hydraulic diameter as small as 25.9 μm. For the convenience of application, a correlation equation for the laminar friction constant in trapezoidal silicon microchannels in terms of the cross-sectional aspect ratio is presented.

* Corresponding author. Tel.: +852-2358-7181; fax: +852-2358-1543.
E-mail address: mepcheng@ust.hk (P. Cheng).

0017-9310/03/$ - see front matter
doi:10.1016/S0017-9310(03)00106-6

Nomenclature

A	cross-sectional area, m^2
D_h	hydraulic diameter, m
f	friction factor
$f\,Re$	friction constant
L	length, m
M	mass flow rate, kg/s
p	pressure, N/m^2
Δp	pressure drop, N/m^2
Re	Reynolds number
T	temperature, °C
$\bar{u}$	average velocity, m/s
W_b	bottom width, m
W_b/W_t	aspect ratio
W_t	top width, m

Greek symbols

ν	viscosity, m^2/s
ρ	density, kg/m^3

Subscripts

d	developing section
i	inlet section
meas	measurement
o	outlet section

2. Experimental description

2.1. Experimental setup

The experimental setup consisted of a pressure tank, a valve, a filter, an inlet reservoir, a test section, an outlet reservoir, and a collecting container. The deionized water in the pressure tank, being pushed by the compressed nitrogen gas, flowed successively through the valve, filter, inlet reservoir, test section, outlet reservoir, and finally was collected in a container. The collecting container was placed on a high precision electronic balance. The mass flow rate of the deionized water was determined by the amount of mass collected per unit time. The temperature and pressure drop of the deionized water through the microchannels were measured by thermocouples and pressure transducers installed at the inlet and outlet reservoirs located at the two ends of the test section. All of the experiments were carried out in a clean room.

The microchannels in the $\langle 100 \rangle$ silicon wafers were fabricated by the wet etching technique. Each of the silicon wafers was then anodically bonded with a thin pyrex glass plate to close the microchannels. A typical cross-section of the microchannels in the $\langle 100 \rangle$ silicon wafers by wet etching is shown in Fig. 1. The channel angle between the side walls and the bottom wall was at 54.7° if the mask plate and the $\langle 100 \rangle$ silicon wafer were aligned perfectly during the fabrication process. Other

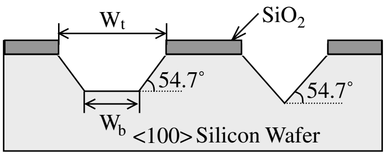

Fig. 1. Cross-section of microchannels by wet etching in $\langle 100 \rangle$ silicon wafer.

geometric parameters (W_t, W_b, D_h) of the 28 microchannels used in this experiment are listed in Table 1, where the microchannels are classified into six different groups N1, N2, N3, N4, N5 and N6. Each of these groups of microchannels was etched in the same wafer but with different etching times, and consequently each group of microchannels had different depths. Note that the triangular and rectangular microchannels are special cases of the trapezoidal microchannels with $W_b/W_t = 0$ and $W_b/W_t = 1$ respectively. Since the channel angle is fixed in the $\langle 100 \rangle$ silicon wafers as mentioned above, the dimensionless parameter, W_b/W_t (the cross-sectional aspect ratio), is the only parameter determining the cross-sectional shape of the microchannels used in the present investigation. Using an atomic force microscope, the relative roughness of all microchannels was measured to be no more than 0.12%. Therefore, the microchannels in the silicon wafers used in this experiment are considered to be *smooth*.

2.2. Data reduction and error analysis

The fully developed pressure drop across the microchannels, Δp, is obtained by

$$\Delta p = \Delta p_{meas} - \Delta p_i - \Delta p_o - \Delta p_d \tag{1}$$

where Δp_{meas} is the total pressure difference measured by the pressure transducers at the inlet and outlet reservoirs, Δp_i, Δp_o, and Δp_d are the minor pressure losses associated with the inlet and outlet as well as in the developing section, respectively. The values of Δp_i, Δp_o and Δp_d were determined by the method described by Shames [8] and Li et al. [9], respectively. A total of 334 data points of pressure drop in the 28 microchannels were measured. It was found that of the 334 data points, 297 data points have total minor pressure losses less than 10%, 34 data points have total minor pressure losses between 10% and 15%, and only 3 data points

Table 1
Geometric parameters and comparison of experimental data with analytical solution [7]

Channel no.	Channel shape	W_t (10^{-6} m)	W_b (10^{-6} m)	W_b/W_t	D_h (10^{-6} m)	Re	$\frac{(f\,Re)_{exp}-(f\,Re)_{analy}}{(f\,Re)_{analy}}$ (%)
N1-100	Trapezoid	100	20.1	0.201	52.5	12.9–408.0	−3.04–0.60
N1-150	Trapezoid	150	70.1	0.467	69.3	17.4–597.9	−0.71–4.70
N1-200	Trapezoid	200	120.2	0.601	78.8	18.7–648.0	2.66–7.53
N1-500	Trapezoid	500	420	0.840	98.1	25.0–883.2	3.67–7.16
N1-1000	Trapezoid	1000	920	0.920	105.3	47.0–959.8	2.25–7.75
N1-4000	Trapezoid	4000	3920	0.980	110.9	14.7–1011.5	1.98–7.58
N2-50	Triangle	50	0	0	25.9	13.7–209.4	−8.61–5.09
N2-100	Trapezoid	100	39.9	0.399	48.7	14.0–247.6	−2.41–2.26
N2-150	Trapezoid	150	89.9	0.599	59.2	14.9–263.4	−2.00–5.11
N2-200	Trapezoid	200	140	0.700	65.0	24.1–310.1	5.36–8.12
N2-500	Trapezoid	500	440	0.880	76.4	31.9–411.1	6.43–9.45
N2-1000	Trapezoid	1000	940	0.940	80.6	14.7–402.5	4.11–10.52
N2-4000	Trapezoid	4000	3940	0.985	83.8	13.5–410.8	4.59–10.03
N3-50	Triangle	50	0	0	25.9	42.4–319.3	−9.80–8.92
N3-100	Triangle	100	0	0	51.7	36.3–730.8	−6.14–3.91
N3-150	Triangle	150	0	0	77.6	76.4–1314.1	−8.68–2.01
N3-200	Triangle	200	0	0	103.4	18.5–1452.2	−10.91–1.54
N3-500	Trapezoid	500	284	0.568	206.6	29.7–1242.9	−3.71–2.50
N3-1000	Trapezoid	1000	784	0.784	252.2	45.0–1417.2	0.43–7.53
N3-2000	Trapezoid	2000	1784	0.892	277.6	52.2–1344.5	1.94–8.12
N3-4000	Trapezoid	4000	3784	0.946	291.0	60.8–1439.1	2.09–7.58
N4-100	Triangle	100	0	0	51.7	20.5–624.0	−8.76–5.42
N4-200	Trapezoid	200	27.2	0.136	105.4	27.7–1418.4	0.36–5.41
N4-500	Trapezoid	500	327	0.654	179.3	37.4–1317.5	3.57–9.29
N4-1000	Trapezoid	1000	827	0.827	209.8	100.3–1328.2	5.85–10.19
N4-4000	Trapezoid	4000	3828	0.957	235.2	62.1–1147.8	4.96–7.35
N5-150	Trapezoid	150	47.4	0.316	76.3	30.3–658.0	−0.71–3.16
N6-500	Trapezoid	500	279	0.559	209.5	42.6–1417.3	−3.14–3.74

have total minor pressure losses between 15% and 22%.

The friction factor is defined as

$$f = \Delta p \cdot \frac{D_h}{L} \cdot \frac{1}{2\rho \bar{u}^2} \tag{2}$$

and the friction constant, $f\,Re$, is defined by

$$f\,Re = \frac{\Delta p \cdot D_h^2}{2\rho v \bar{u} L} \tag{3}$$

where v is the viscosity of deionized water which is a function of temperature, and $\bar{u} = M/\rho A$ is the average velocity of deionized water with M, ρ, A being the mass flow rate, water density and cross-sectional area of a microchannel, respectively. The above expression in terms of the mass flow rate M is

$$f\,Re = \frac{\Delta p \cdot A \cdot D_h^2}{2v \cdot M \cdot L} \tag{4}$$

According to Eq. (4), the error of the friction constant, $f\,Re$, is caused by measurement errors of Δp (0.68%), A (3.67%), D_h (1.83%), M (1.69%), L (0.37%), and $v(T)$ (1.01%). Performing the standard error analysis, the maximum uncertainty in determining $f\,Re$ in this experiment is 11%.

3. Experimental results and discussion

3.1. Effect of cross-sectional shape on friction factors

Figs. 2–5 give the experimental results of friction constant for the laminar flow of deionized water in smooth microchannels of silicon wafers #N1, N2, N3 and N4, respectively. It can be seen from these figures that the laminar friction constants of these microchannels, having a triangular or trapezoidal cross-section, deviate greatly from the classical value of $f\,Re = 16$ for a circular tube. For the triangular microchannels (with $W_b/W_t = 0$) such as N2-50 in Fig. 3, N3-50/100/150/200 in Fig. 4, and N4-100 in Fig. 5, the friction constants are much lower than that of a circular tube. While, for the rest of the microchannels with trapezoidal cross-sections, the friction constants could be lower or higher than that of circular tubes depending on the values of W_b/W_t. Within the experimental range of $D_h = 25.9$–291.0 μm and $W_b/W_t = 0$–0.985, the laminar friction

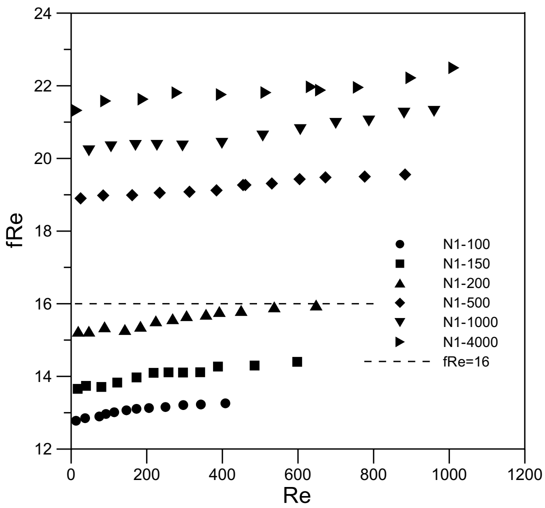

Fig. 2. Friction constant of microchannels in wafer #N1.

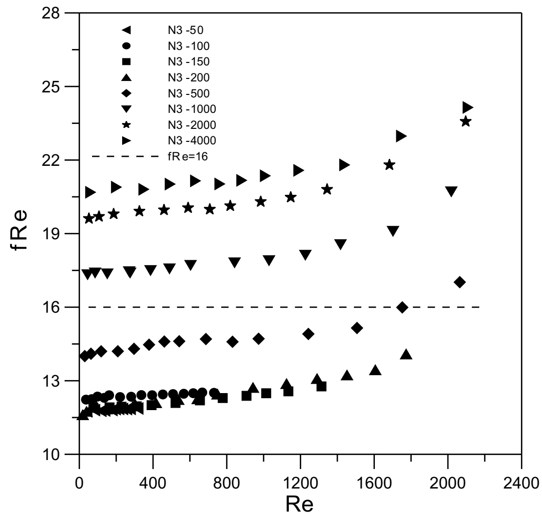

Fig. 4. Friction constant of microchannels in wafer #N3.

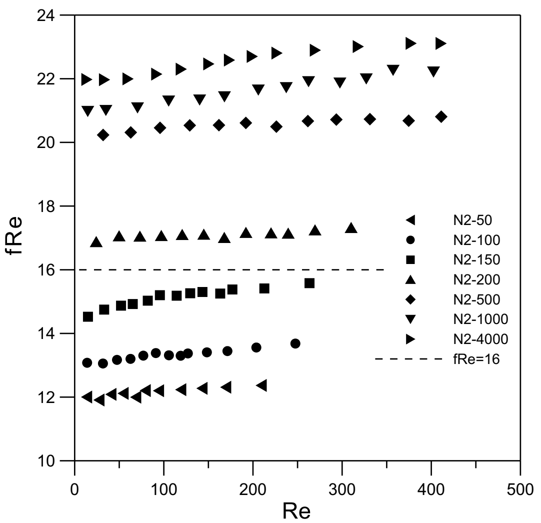

Fig. 3. Friction constant of microchannels in wafer #N2.

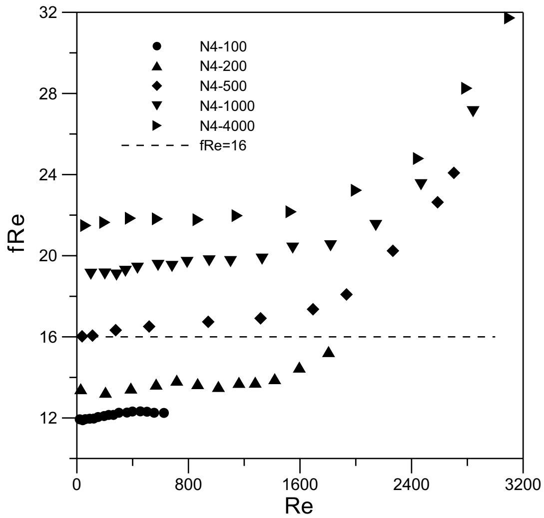

Fig. 5. Friction constant of microchannels in wafer #N4.

constant $f\,Re$ of the trapezoidal channels increases with the increase in aspect ratio W_b/W_t, with a minimum value of 11.61 at $W_b/W_t = 0$ (a triangular channel) and a maximum value of 23.11 at $W_b/W_t = 0.985$. That is, the laminar friction constant in a highly flat trapezoidal microchannel ($W_b/W_t \approx 1$) can be up to two times as those in the triangular microchannel, and this should be taken into consideration when designing microchannels in $\langle 1\,0\,0 \rangle$ silicon-based microsystems.

Fig. 6 shows the effect of the cross-sectional aspect ratio on the friction constant in three sets of trapezoidal microchannels having the hydraulic diameters of $D_h =$ 76, 105, 209 μm. It is shown that the microchannels, having the same hydraulic diameter but with different cross-sectional shapes, may have very different values of friction constant. The data of the friction constant for $D_h = 76$ μm are represented by open circles and solid circles for $W_b/W_t = 0.316$ and 0.880 respectively. For the aspect ratio of 0.316 (represented by the open circles), the friction constant varies from 13.10 to 13.61 as the Reynolds number is increased while the friction constant for the aspect ratio of 0.880 (represented by solid circles) varies from 20.23 to 20.80 as the Reynolds number is

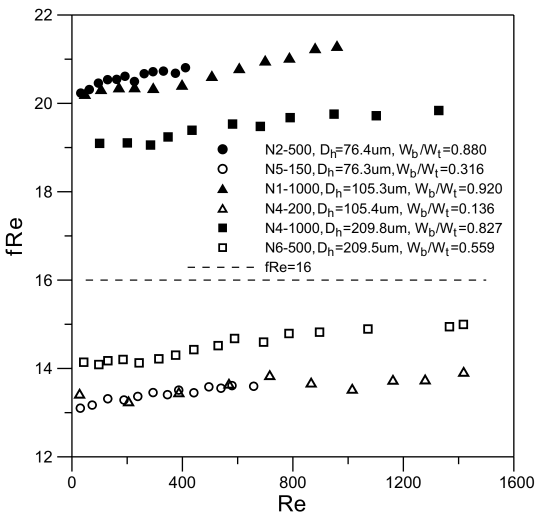

Fig. 6. Effect of aspect ratio on friction constant of microchannels with same hydraulic diameters.

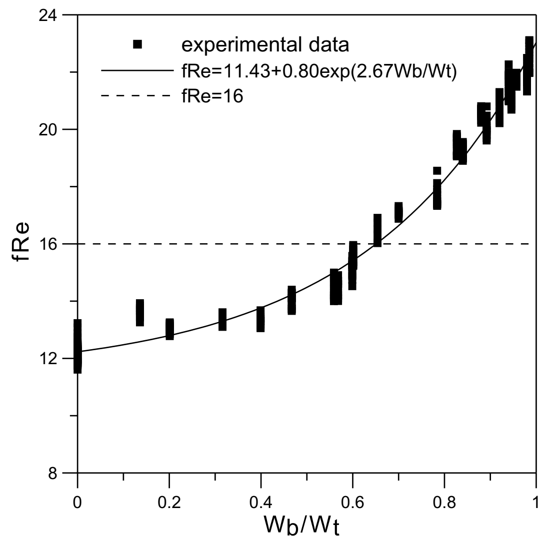

Fig. 7. Comparison of experimental data with correlation equation.

increased within the laminar range. Similarly, the friction constants for $D_h = 105$ μm are represented by open and solid triangles corresponding to the aspect ratios of 0.136 and 0.920 respectively. It is shown that the increase in aspect ratio resulting in an increase of the friction constant from 13.25–13.92 to 20.21–21.30. Finally, it is shown that the friction constant for $D_h = 209$ μm increases from 14.08–14.99 to 19.05–19.83 corresponding to an increase of the cross-section aspect ratio from 0.559 to 0.827. It is evident that the friction constant increases with an increase in the cross-sectional aspect ratio even though the hydraulic diameter is the same. This implies that it is the shape and not the microdimension that had caused the deviations in the friction constant of the noncircular microchannels as reported previously by some researchers.

3.2. Correlation of laminar friction constant in terms of cross-sectional aspect ratio

Based on the 334 sets of experimental data obtained from this experiment, the following equation was obtained to correlate the laminar friction constant of the trapezoidal microchannels in terms of the cross-sectional aspect ratio (W_b/W_t):

$$f\,Re = 11.43 + 0.80\exp(2.67W_b/W_t) \quad (5)$$

A comparison of Eq. (5) with experimental data is presented in Fig. 7, where the relative deviation of the experimental data with respect to the correlation equation is no more than 9.7%. It is also shown that the friction constant $f\,Re$ of a trapezoidal microchannel is less than 16 for $W_b/W_t < 0.65$, and is greater than 16 for $W_b/W_t > 0.65$. Eq. (5) can be used to predict the friction constant for laminar flow of water in a smooth microchannel in ⟨1 0 0⟩ silicon wafers formed by wet etching.

3.3. Applicability of Navier–Stokes equations in microchannels

Ma and Peterson [7] have obtained the following analytical expression for friction constant of a laminar fully developed incompressible flow in microchannels with two arbitrary boundaries under no-slip boundary condition:

$$f\,Re = \frac{4[\int_0^{2\phi}[f_2^2(\theta) - f_1^2(\theta)]\,d\theta]^3}{D} \quad (6)$$

where $D = [f_2(0) - f_1(0) + f_2(2\phi) - f_1(2\phi) + \int_0^{2\phi}[f_1(\theta) + f_2(\theta)]\,d\theta]^2 \int_0^{2\phi}\int_{f_1(\theta)}^{f_2(\theta)} f_1^2(\theta)F(\theta,r)r\,dr\,d\theta$, where the definitions of θ, ϕ, and $F(\theta,r)$ can be found from their paper [7], and the functions $f_1(\theta)$ and $f_2(\theta)$ depend on the specific geometry under consideration. For the case of a trapezoidal cross-section in the ⟨1 0 0⟩ silicon wafer shown in Fig. 1, $f_1(\theta)$ and $f_2(\theta)$ are given by

$$f_1(\theta) = \frac{r_1\cos\phi}{\cos(\theta - \phi)} \quad \text{and} \quad f_2(\theta) = \frac{r_2\cos\phi}{\cos(\theta - \phi)} \quad (7)$$

where $r_1 = W_b/(2\cos 54.7°)$, $r_2 = W_t/(2\cos 54.7°)$, and $\phi = (180° - 2 \times 54.7°)/2 = 35.3°$.

Fig. 8 shows the comparison of friction constants between experimental data in the laminar flow range and the analytical values computed from Eqs. (6) and (7).

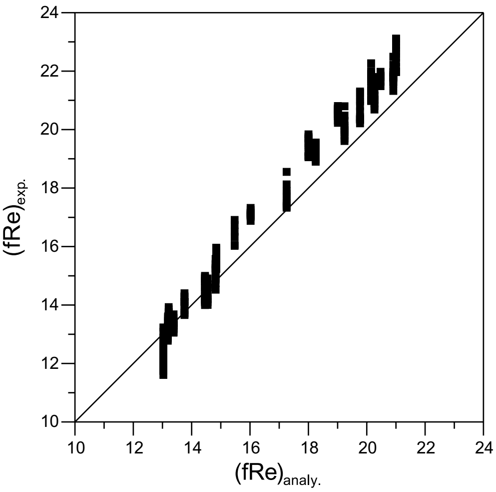

Fig. 8. Comparison of experimental data with Ma and Peterson's analytical solution [7].

The relative deviations of experimental data from those of analytical solutions at the range of Reynolds number for which the experiments were performed are also listed in Table 1. It is shown that the experimental results are in reasonable agreement with the laminar friction model given by Ma and Peterson [7], with the relative deviation ranging from −10.9% to +10.5%. Therefore, it can be concluded that the Stokes flow theory is applicable for the trapezoidal microchannels having hydraulic diameters as small as 25.9 μm.

3.4. Transition from laminar to turbulent flow

Limited by the maximum allowable pressure in the tank, the transition from laminar to turbulent flow was observed only for the microchannels having a large hydraulic diameter. According to Figs. 4 and 5, the transition to turbulent flow occurred at about $Re = 1500$–2000 for smooth microchannels with $D_h = 103.4$–291.0 μm.

4. Conclusions

The following conclusions are obtained from this experimental investigation:

1. The experimental data for friction constants of deionized water in smooth microchannels agree within ±11% of the analytical solution based on the Stokes flow theory. It appears that the Navier–Stokes equations are applicable for the deionized water flow in *smooth* silicon microchannels having hydraulic diameter as small as 25.9 μm.
2. Measurements show that the friction constant of liquid flowing in microchannels, having the same hydraulic diameter but with different cross-sectional shapes, can be very much different. This is because the cross-sectional shape of the microchannels has a significant effect on the friction factor. Thus, previous experimental results on the laminar friction constants of liquid through noncircular microchannels in silicon wafers, being higher or lower than the classical value of 16 or 64, may be owing to the fact that microchannels of different shapes were used in their experiments.
3. Based on the 334 experimental data points, a correlation equation for the laminar friction constant of deionized water flowing in smooth $\langle 100 \rangle$ silicon microchannels in terms of the cross-sectional aspect ratio is presented. It is shown that the friction constant increases with the increase of cross-sectional aspect ratio. It is also found that the friction factor $f\,Re$ is less than 16 for $W_b/W_t < 0.65$, and is greater than 16 for $W_b/W_t > 0.65$.
4. Transition from laminar to turbulent flow occurred at $Re = 1500$–2000 in microchannels having triangular or trapezoidal cross-section with $D_h = 103.4$–291.0 μm.

Acknowledgements

The authors gratefully acknowledge the support of this work through grant no. HIA98/99.EG04.

References

[1] P. Wu, W.A. Little, Measurement of friction factors for the flow of gases in very fine channels used for microminiature Joule–Thomson refrigerators, Cryogenics 23 (1983) 273–277.
[2] X.N. Jiang, Z.Y. Zhou, X.Y. Huang, C.Y. Liu, Laminar flow through microchannels used for microscale cooling systems, in: Proceedings of the 1997 IEEE/CPMT Electronic Packaging Technology Conference, 1997, pp. 119–122.
[3] X.F. Peng, G.P. Peterson, B.X. Wang, Frictional flow characteristics of water flowing through rectangular microchannels, Exp. Heat Transfer 7 (1994) 249–265.
[4] B. Xu, K.T. Ooi, N.T. Wong, C.Y. Liu, Liquid flow in microchannels, in: Proceedings of the 5th ASME/JSME Thermal Engineering Conference, 1999, pp. 6214–6220.
[5] J.M. Cuta, C.E. McDonald, A. Shekarriz, Forced convection heat transfer in parallel channel array microchannel heat exchanger, in: ASME Proceedings, PID-Vol. 338, Advances in Energy Efficiency, Heat/Mass Transfer Enhancement, 1996, pp. 17–23.
[6] D. Pfund, D. Rector, A. Shekarriz, A. Popescu, J. Welty, Pressure drop measurements in a microchannel, AICHE J. 46 (8) (2000) 1496–1507.

[7] H.B. Ma, G.P. Peterson, Laminar friction factor in microscale ducts of irregular cross section, Microscale Thermophys. Eng. 1 (1997) 253–265.
[8] I.H. Shames, Fluid Mechanics, McGraw-Hill Inc., 1992, pp. 368–371.
[9] Z.X. Li, D.X. Du, Z.Y. Guo, Experimental study on flow characteristics of liquid in circular microtubes, in: Proceedings of the International Conference on Heat Transfer and Transport Phenomena in Microscale, Banff, Canada, October 2000, pp. 162–167.